THE ANATOMICAL RECORD 296:759–773 (2013)

# Cell Proliferation Patterns in Early Zebrafish Development

**MARIO A. MENDIETA-SERRANO, DENHI SCHNABEL, HILDA LOMELÍ, AND ENRIQUE SALAS-VIDAL***

Departamento de Fisiología Molecular y Genética del Desarrollo, Instituto de Biotecnología, Universidad Nacional Autónoma de México, Colonia Chamilpa, Cuernavaca, Morelos, C.P., 62210, México

ABSTRACT

Although cell proliferation is an essential cell behavior for animal development, a detailed analysis of spatial and temporal patterns of proliferation in whole embryos are still lacking for most model organisms. Zebrafish embryos are particularly suitable for this type of analysis due to their transparency and size. Therefore, the main objective of the present work was to analyze the spatial and temporal patterns of proliferation during the first day of zebrafish embryo development by indirect immunofluorescence against phosphorylated histone H3, a commonly used mitotic marker. Several interesting findings were established. First, we found that mitosis metasynchrony among blastomeres could begin at the 2- to 4-cell stage embryos. Second, mitosis synchrony was lost before the midblastula transition (MBT). Third, we observed a novel pattern of mitotic clusters that coincided in time with the mitotic pseudo "waves" described to occur before the MBT. Altogether, our findings indicate that early development is less synchronic than anticipated and that synchrony is not a requirement for proper development in zebrafish. Anat Rec, 296:759–773, 2013. 

**Key words: proliferation; asynchrony; *Danio rerio*; phosphorylated histone H3; patterns; mitotic clusters**

Embryonic development requires the coordination of fundamental cellular behaviors such as proliferation, death, migration, and differentiation to achieve embryonic patterning and morphogenesis. The understanding of the molecular mechanisms that control these behaviors during development has rapidly advanced in recent years. By contrast, we still lack detailed descriptions of the spatial and temporal patterns of different cell dynamics such as proliferation or cell death. The identification of these patterns is required for a comprehensive analysis of normal and pathological development, as well as for comparative studies throughout evolution.

Cell proliferation is triggered at the onset of development and is required to generate sufficient cell numbers for proper embryogenesis. Cell proliferation patterns have been described in diverse animal models in different degrees of detail. For example, in the free-living nematode *Caenorhabditis elegans*, embryonic cell lineages are highly invariant and can be traced from the zygote to the hatched larva because of the small number of

Additional Supporting Information may be found in the online version of this article.

Grant sponsor: IXTLI-UNAM; Grant number: IX201110; Grant sponsor: DGAPA-UNAM; Grant numbers: IN219309-3; IN205612; IN204712.

*Correspondence to: Enrique Salas-Vidal, Departamento de Fisiología Molecular y Genética del Desarrollo, Instituto de Biotecnología, Universidad Nacional Autónoma de México, Avenida Universidad #2001, Colonia Chamilpa, Cuernavaca, Morelos, C.P. 62210, México. E-mail: esalas@ibt.unam.mx

Received 30 July 2012; Accepted 20 February 2013.

DOI 10.1002/ar.22692

Published online 1 April 2013 in Wiley Online Library (wileyonlinelibrary.com).

cells generated during embryogenesis (671 cells in total) (Sulston et al., 1983). By contrast, the other most commonly used model organisms do not exhibit invariant patterns of cell proliferation. In the fruit fly *Drosophila melanogaster*, development begins with rapid and metasynchronous mitotic "waves" that traverse the syncytial embryo. After the 14th cell cycle, the embryo cellularizes, interphase extends, asynchrony begins (Edgar and O'Farrell, 1989) and cell mitotic domains with different developmental fates can be observed (Foe, 1989). In the amphibian *Xenopus laevis*, synchronous cleavage of blastomeres occurs from fertilization up to the tenth to twelfth cell cycle; thereafter, cell division become asynchronous in embryos at the midblastula transition (MBT), with an apparently random distribution of mitotic nuclei (Saka and Smith, 2001). Although in *Xenopus*, mitotic domains have also been observed after the MBT in different tissues, they are not as extensive and well-defined in time and space as the mitotic domains described in *Drosophila*.

In zebrafish (*Danio rerio*), classical studies indicate that synchronous cleavages occur until the MBT, when the cell cycle lengthens and cell division becomes asynchronous. In spite of these observations, many embryos show global metasynchrony before cycle 10 (Kane and Kimmel, 1993). More recent studies have demonstrated that cell divisions are metasynchronous at the transition of the 4- to 8-cell stage, presenting a delay among blastomere divisions that increases during subsequent cleavages (Olivier et al., 2010) and leading to mitotic asynchrony by the 512 to 1k-cell stage (Kane and Kimmel, 1993). This evidence suggests that early cell cycle metasynchrony before the MBT has been largely underestimated. We considered that early patterns of proliferation should be analyzed more thoroughly and that a more conventional analysis of representative embryos could be particularly useful as a reference of patterns and for the study of different drug effects and mutants that disturb early development. In the present study, we focused on the analysis of global mitotic patterns and generated detailed graphical references for the normal patterns during the first day of zebrafish development. Several interesting findings were established. First, we found that as early as the two-cell stage, zebrafish embryos exhibit mitotic metasynchrony among blastomeres in ~10% of embryos. Second, the quantified nuclei number and mitotic indexes differ from those predicted by the classical synchronization model from the 16-cell to 512-cell stage. Third, we observed a novel pattern of mitotic clusters of interphase cells coinciding in time with the mitotic pseudo "waves" reported at these stages. The patterns described in the present work prompt interesting questions about the contribution of cell proliferation to early development while generating a graphical reference for the comparative analysis of the occurrence of proliferation.

## MATERIALS AND METHODS

### Fish Maintenance and Strains

Wild-type zebrafish (*Danio rerio*) embryos were obtained from natural crosses and raised at 28°C. Embryo stages were determined by morphological criteria according to Kimmel et al. (1995). Cleavage and early blastula embryos up to 512-cell stage were more precisely assigned to a particular stage by counting the nuclei and/or the segregated anaphase sister chromosomes as described below. Zebrafish were handled in compliance with local animal welfare regulations and approved by Comité de ética (Instituto de Biotecnología, UNAM).

### Chemical Treatment of Zebrafish Embryos

Compounds for chemical treatments were diluted in anhydrous DMSO (276855, Sigma-Aldrich). Compounds and stock concentrations were aphidicolin (10 mg/mL, A0781, Sigma-Aldrich) and nocodazole (10 mg/mL, M1404, Sigma-Aldrich). For each treatment, 10 zebrafish embryos at 24 h postfertilization were incubated at 28°C in egg water for 6 h in 48-well plates. A 3 μL volume of each compound stock solution was added to a total volume of 300 μL at the beginning of the incubation. Control embryos were treated with DMSO alone at a final concentration of 1% (v/v) and processed as described below.

### Immunofluorescence and Immunohistochemistry

Whole-mount immunostaining in zebrafish embryos was used to determine the cell proliferation patterns as previously described for mouse preimplantation embryos (Salas-Vidal and Lomeli, 2004), with slight modifications. Embryos were freshly collected and fixed overnight (o.n.) at 4°C in 4% PFA in PBS, washed 3 times in blocking buffer (PBS, BSA 0.1%, TX100 1%), manually dechorionated and blocked 2 h in blocking buffer at room temperature. The blocking step and all following steps were done with soft constant shaking. The primary antibody, rabbit IgG, antiphosphorylated histone H3 (sc-8656-R, Santa Cruz Biotechnology), was diluted 1:100 in blocking buffer (final concentration 2 μg/mL), and embryos were incubated in this solution at 4°C o.n. Subsequently, embryos were washed 3 times in blocking buffer and incubated in goat antirabbit Alexa Fluor 647 (Molecular Probes) solution 1:100 in blocking buffer for 1 h at room temperature. Embryos were washed 3 times and counterstained for 1 h at room temperature with SYTOX Green (Molecular Probes) diluted 1:2000 in blocking buffer to visualize DNA and nuclei. The embryos were then washed 3 times and mounted in 2.5% methyl cellulose or in low melting point agarose in PBS for epifluorescence or for confocal laser scanning microscopy.

Freshly fixed zebrafish embryos younger than the 1k-cell stage were treated with 0.4 mg/mL RNase (Roche) in blocking buffer for 1–2 h at 37°C, washed twice in blocking buffer and double-stained by the procedure described above (Supporting Information Fig. 1).

For immunohistochemistry, embryos were processed as for inmunostaining, except that after the o.n. incubation with the primary antiphosphorylated histone H3 antibody, embryos were processed with the R.T.U. Vectastain Universal Quick Kit (PK-7800, Vector) and developed in diaminobenzidine with nickel contrast substrate (SK-4100, Vector).

### Confocal Laser Scanning Microscopy

Zebrafish embryos stained with the specified fluorescent dyes were visualized on a Zeiss LSM 510 META

confocal inverted microscope (Carl Zeiss, Jena, Germany) with a PlanNeofluar 10× (numeric aperture 0.3) objective and for the measurement of region-specific mitotic indexes with a PlanNeofluar 20× (numeric aperture 0.5) objective or a PlanNeofluar 40× (numeric aperture 0.75). Some images were obtained in a FluoView FV1000 confocal microscope or a Mai Tai Deep See Spectra-Physics Multi-photon system coupled to an up-right BX61WI Olympus microscope with a Plan FLN 10X (numeric aperture 0.3) objective or a XLPlanN WMP 25X (numeric aperture 1.05) objective. Double-stained embryos were simultaneously excited with 488 and 633 nm light and visualized. The pinhole aperture was maintained at 105. Serial optical sections were obtained with a *z*-step of 10 μm. Images were processed with the public domain software ImageJ (Abramoff et al., 2004), the LSM Image Browser from Zeiss and Adobe Photoshop.

### *In Vivo* Labeling of Embryo Nuclei and Visualization

To vitally stain embryo nuclei, fertilized eggs before the formation of the first cell were injected in the yolk with 1 nL of a 0.5 mM solution of SYTOX Green (Invitrogen) diluted in Danieu buffer. After reaching the 1-cell stage, the injected embryos were inspected under a fluorescent microscope to select embryos with stained nuclei. Then, the embryos were observed on an Axioscope upright compound microscope (Zeiss, Germany) with a PlanNeofluar 10× (aperture 0.30) objective. Image time series at 1 min intervals were acquired with a CoolSNAP cfd CCD camera (Roper Scientific, Tucson, AZ) controlled by MicroManager 1.5 software (NIH) and analyzed with the public domain software ImageJ.

### Image Analysis and Mitotic Index Determination

Confocal image series were processed by ImageJ 1.46a. Nuclei were counted with the 3D Objects Counter plugin from the 1 to 512-cell stages, stages during which the SYTOX Green nuclei and PH3-positive nuclei could be resolved. In more advanced stages whole embryos were not analyzed because it was not possible to spatially resolve the SYTOX Green-stained nuclei. Region specific mitotic indexes were determined in higher magnification image stacks, in which nuclei were resolved. This was performed in the ventral and dorsal regions of 70% epiboly embryos and dorsal views of somite stage embryos. Original stacks, generated object maps and statistics are available upon request. Three-dimensional renderings were generated with FluoRender software (http://www.sci.utah.edu/software/127-fluorender.html).

## RESULTS

### Visualization of Mitosis in Whole Zebrafish Embryos

Mitotic nuclei were visualized in whole zebrafish embryos by indirect immunofluorescence using a primary antibody specific for the phosphorylated form of histone H3 (PH3) at serine 10 (Hendzel et al., 1997). This antibody was used previously in *Xenopus* and zebrafish (Saka and Smith, 2001; Zhang et al., 2008). As the secondary antibody, an antirabbit antibody coupled to the fluorophore Alexa 647 was used, and embryos where costained with SYTOX Green. This combination of fluorophores permitted the simultaneous visualization and spectral resolution of both signals by confocal microscopy (Figs. 1 and 2). The confocal images revealed that the PH3 antibody specifically stained mitotic nuclei (Fig. 1) but not interphase nuclei (Fig. 3E). By contrast, SYTOX Green stained DNA served as a reference for embryo structure (Fig. 2).

To further confirm that the PH3 primary antibody specifically recognized mitotic nuclei, 24 h zebrafish embryos were incubated for 6 h in the presence of either nocodazole or aphidicolin and compared with control embryos incubated with vehicle only (1% DMSO). Both nocodazole and aphidicolin are known to arrest zebrafish cells at specific stages of the cell cycle (mitosis and synthesis, respectively) (Urbani et al., 1995; Ikegami et al., 1997; Murphey et al., 2006). As expected, nocodazole-treated embryos exhibited an increase in PH3-positive nuclei as compared to control embryos. In contrast, aphidicolin-treated embryos exhibited a dramatic decrease in PH3-positive nuclei (Supporting Information Fig. 2).

Zebrafish embryos were collected and classified by morphological criteria according to Kimmel et al. (1995), fixed and processed to analyze the patterns of proliferation in whole mount from the 1-cell stage (0.75 h postfertilization (hpf)) up to 28 somite stage (∼31 hpf) of development. In the following sections, the results are presented by periods to facilitate the description.

### Cell Division Patterns at the Cleavage Period

During early development in many animal species, rapid and synchronous cleavages occur after the first cell forms, generating a large population of blastomeres. In zebrafish, classical studies indicate that global synchronous cleavages occur up to the 10th cell cycle at the onset of the MBT, although metasynchronous "waves" of mitosis have been described to occur before the MBT (Kane and Kimmel, 1993; Kimmel et al., 1995). More recently, Olivier et al. (2010) imaged and reconstructed cell lineages for the first 10 cell cycles in unlabeled zebrafish embryos and found that cell division begins to drift out of synchrony at the transition of the 4- to 8-cell stage. Therefore, if the synchronization drift begins around this stage, it should be possible to detect the synchronization drift with mitosis markers.

In the analysis of phosphorylated histone H3 (PH3), we found both 4-cell and 8-cell stage embryos were synchronized at mitosis (Figs. 1 and 3A–C) or at interphase (Fig. 3D–F). In agreement with the observation of Olivier et al., we also found embryos at the 4-cell stage that presented their nuclei with a shift in synchrony in mitosis (Fig. 3G, compare nuclei 1 and 3 with 2 and 4).

In a further analysis of the PH3 marker by nonfluorescent immunohistochemistry (Fig. 4), we found that this synchrony shift was observed in embryos as early as the 2-cell stage. With the nonfluorescent processed samples, it was possible to quantify this observation in embryos at the 1- ($n = 40$), 2- ($n = 91$), and 4-cell ($n = 45$) stages. The majority were found to be at interphase (82.5%, 55%, and 58%, respectively) rather than mitosis (17.5%, 45%, and 42%, respectively) at the 1-, 2-, and 4-cell stages. Interestingly, 10.8% of the mitotic 2-cell

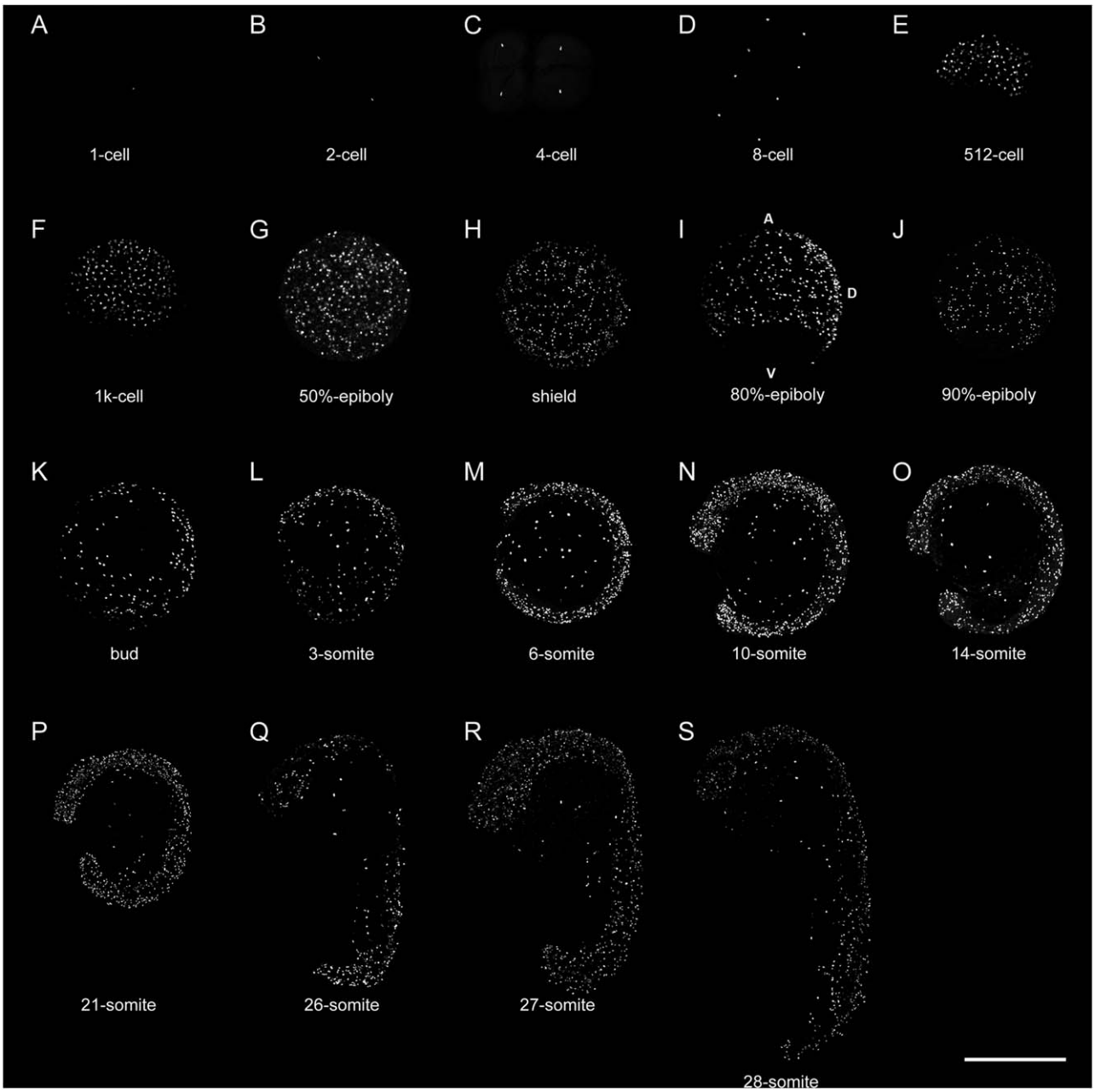


Fig. 1. Proliferation patterns during early zebrafish development as detected by phosphorylated histone H3 (PH3) immunofluorescence and visualized by laser confocal microscopy. (**A**) 1-cell. (**B**) 2-cell. (**C**) 4-cell. (**D**) 8-cell. (**E**) 512-cell. (**F**) 1k-cell. (**G**) 50%-epiboly. (**H**) shield. (**I**) 80%-epiboly. (**J**) 90%-epiboly. (**K**) bud. (**L**) 3-somite. (**M**) 6-somite. (**N**) 10-somite. (**O**) 14-somite. (**P**) 21-somite. (**Q**) 26-somite. (**R**) 27-somite. (**S**) 28-somite. Lateral left side views with the animal pole to the top are shown from 512- to 1k-cell stage and from 80%-epiboly to 28-somite stages. At (A–D) 1-cell to 8-cell, (G) 50%-epiboly, and (H) shield stage embryos, animal pole views are shown. Scale bar 500 μm.

embryos exhibited differences in staining for PH3, with only one positive blastomere (Fig. 4), while 46% of the mitotic 4-cell stage embryos presented one negative or faintly stained nuclei (Fig. 4).

These PH3 staining differences were less obvious in the embryos visualized by confocal microscopy (Fig. 5). Therefore, to confirm the synchrony shift, we imaged the nuclear dynamics in living embryos during the first two cell cycles by staining the DNA. Embryos before or at the 1-cell stage were injected in the yolk with SYTOX Green as described previously (D'Amico and Cooper, 2001). We found that in 6 of 10 2- or 4-cell stage embryos, chromosome segregation begins first at one blastomere, indicating that metasynchrony can be observed in living embryos (Fig. 6, white arrowhead) and more frequently found in part because embryos are imaged every minute. Interestingly, we also observed that cytokinesis in this particular embryo began earlier

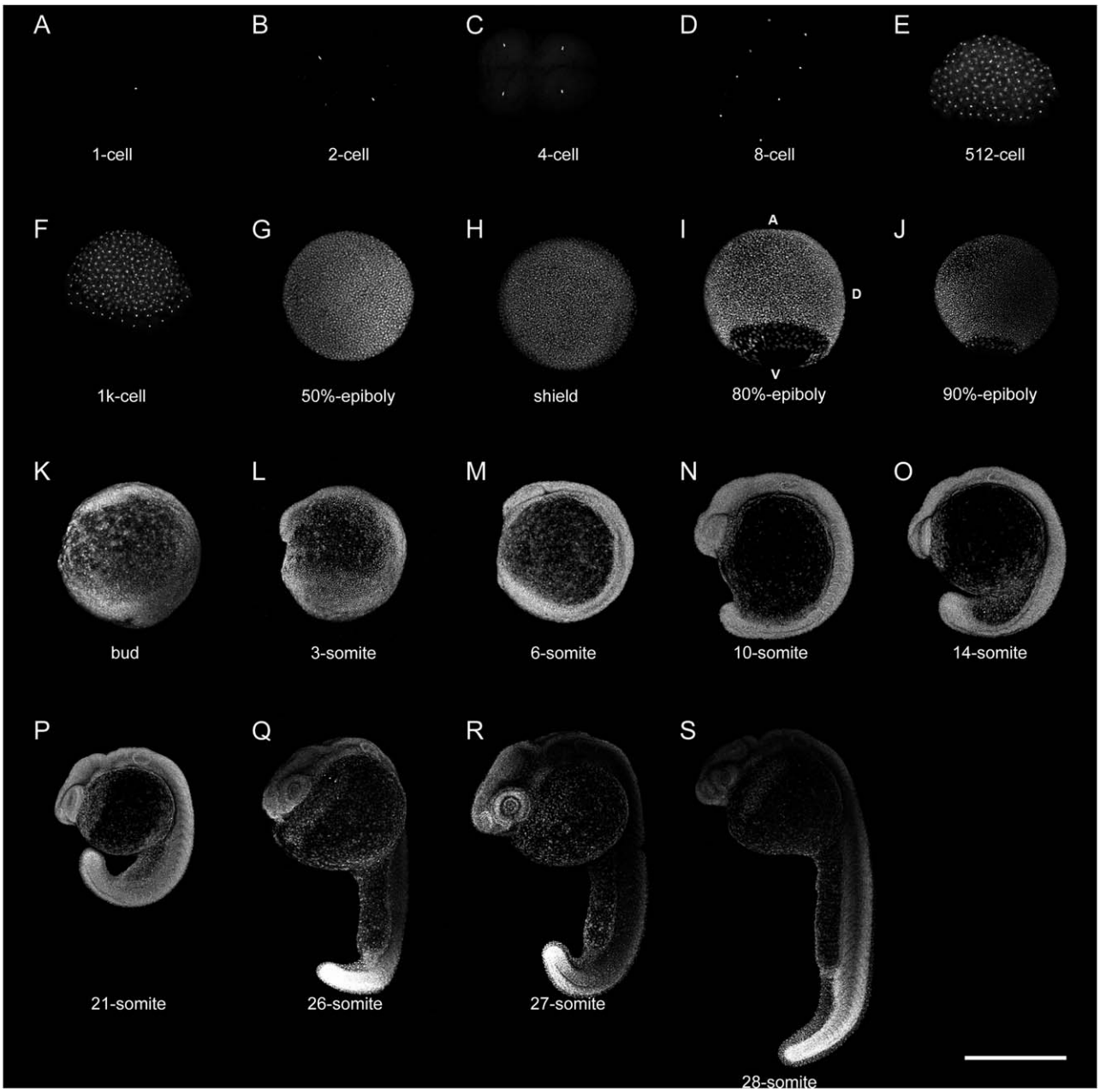


Fig. 2. Nuclei distribution patterns during early zebrafish development. DNA and nuclei were visualized in whole SYTOX Green stained embryos by laser confocal microscopy. The images in this figure are complementary to images shown in Fig. 1. Scale bar 500 μm.

in one blastomere (Fig. 6, small white arrow). Unfortunately, SYTOX Green injected embryos exposed often to fluorescent light stop development at 4- or 8- cell stage. This occurs also in embryos imaged by confocal or multiphoton microscopy (not shown). However, in another experimental group, where embryo exposure to light was minimum, only two or three times to detect asynchrony, embryos were able to advance in development up to 30% of epiboly (Supporting Information Fig. 3). Moreover, embryos from the same injection experiments not exposed to light at all developed normally by 24 h and present all nuclei stained (Supporting Information Fig. 4) indicating that is the exposure to light of SYTOX Green injected embryos what causes damage since non-injected embryos exposed to light develop normally (Not shown). Interestingly, by the 32- to 64-cell stage, differences in the PH3 mitosis marker are clearly observed among positive nuclei, highlighting the synchronization shift (Fig. 5G–J). In addition, in some embryos, the PH3 staining pattern also suggests that the proliferation pseudo "wave" could begin around this stage (Fig. 5H, arrow).

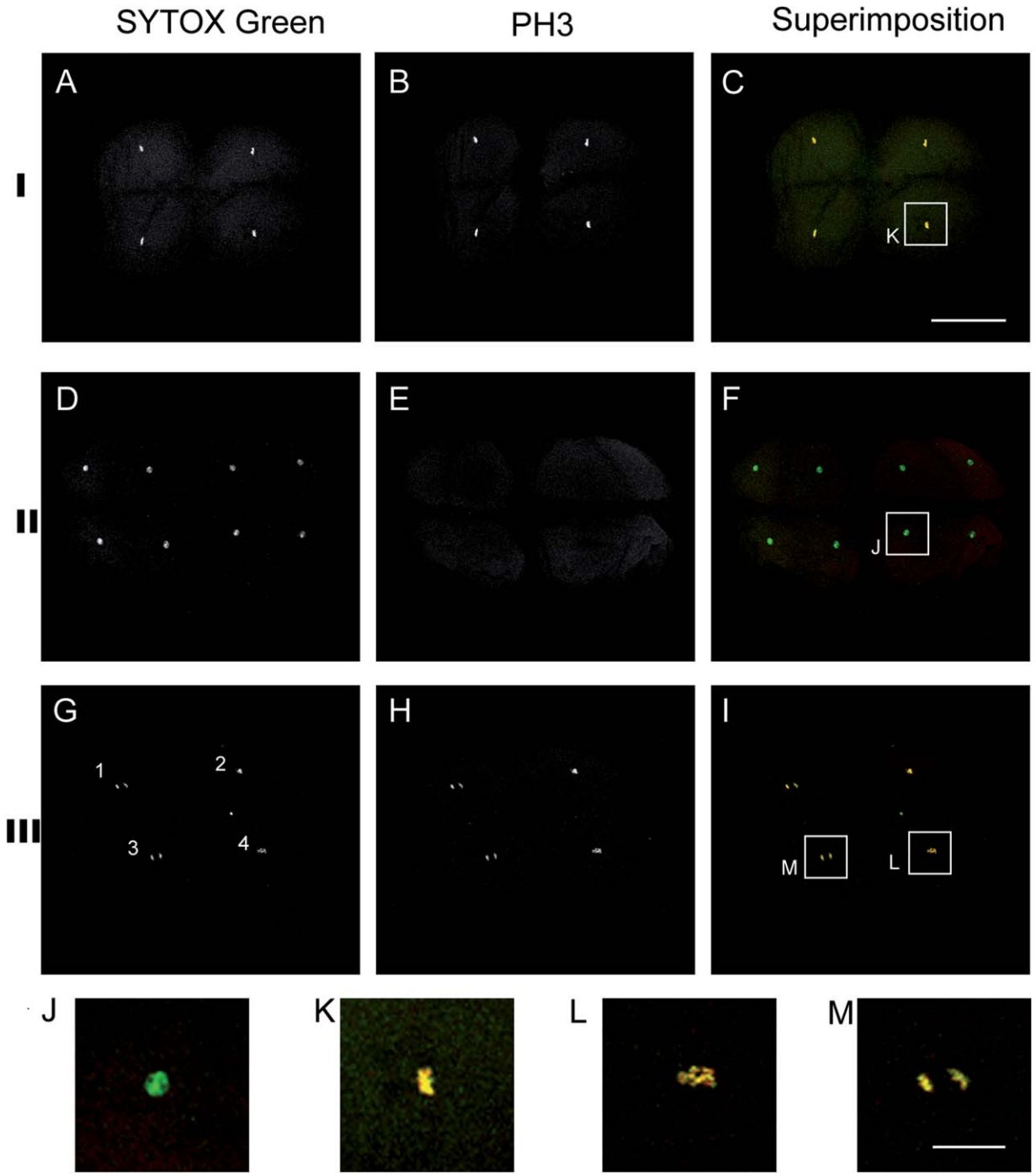


Fig. 3. Nuclei and PH3 immunofluorescence patterns in zebrafish embryos at the 4- to 8-cell stage. (**A**, **D**, and **G**) SYTOX Green stained embryos. (**B**, **E**, and **H**) PH3 immunofluorescence. **I:** 4-cell stage embryo with four nuclei positive for PH3. **II:** 8-cell stage embryo with eight nuclei (D) all negative for PH3 (E, **F**). **III:** 4-cell stage embryo with blastomeres at different stages of mitosis (G) and all their nuclei positive for PH3 (H, I). Inserts (**J–M**) show nuclei at different stages of the cell cycle: (J) interphase, (K) metaphase, (L) early anaphase, (M) late anaphase. Animal views are shown. Nuclei are in green, PH3 marker in red. Scale bar 200 μm in C; 50 μm in M.

## Cell Division Patterns at the Blastula Period

The blastula period comprises the late 7th cycle up to the late 13th cycle. Metasynchronous cleavages have also been described during this period, presenting a pseudo "wave" pattern that begins near the animal pole and extending into the rest of the embryo, with the marginal cells entering last (Kimmel et al., 1995; Keller et al., 2008; Olivier et al., 2010). We found evidence of the pseudo "wave" pattern in embryos at the 128-cell stage (Fig. 5L) and up to the 1k-cell stage (Fig. 7A–F).

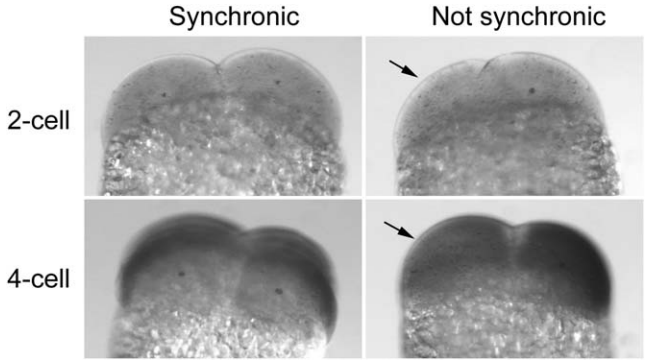


Fig. 4. PH3 immunohistochemistry patterns during cleavage period in 2- and 4-cell stage zebrafish embryos. Lateral views are shown. Synchronic patterns of mitosis (Left column) in 2- and 4-cell stage embryos show all their nuclei positive for the PH3 marker. Nonsynchronic patterns of mitosis (right column) in 2- and 4-cell stage embryos, in which the blastomeres negative for the PH3 marker, are indicated by the arrow. Positive nuclei show a dark staining and round shape.

In 512- and 1k-cell embryos, animal pole blastomeres were positive for the mitosis marker, while the most vegetally positioned cells were negative (Fig. 7A–C). We present a 1k-cell stage embryo in which the "wave" has extended to the whole embryo, including cells of the newly formed YSL (Fig. 7D–F). However, the pseudo "wave" is not a completely homogeneous pattern because clusters of PH3-negative cells, possibly representing clonal or regional synchronization at interphase, were observed in regions of the blastoderm beginning at 128-cell embryos (Figs. 7E, asterisks and 5L). Additionally, we found 1k-embryos synchronized at interphase, and all (embryo and YSL) nuclei negative for PH3 (Fig. 7G–I) exhibited rounded nuclear shapes characteristic of interphase (i insert in 7I). By contrast, embryos with full synchronization at mitosis were never observed at this stage.

During the course of our experiments, we also noticed that nuclei numbers did not always correspond to those expected for a synchronous, exponential division. To document this observation in detail, we counted the total nuclei number or the segregated anaphase sister chromosomes and determined the mitotic index in embryos from the 1- to 512-cell stage.

The majority of embryos between 1- and 8-cells presented the expected nuclei/cell number and a mitotic index of 1 or 0, corresponding to mitosis or interphase. However, from the 16- to 512-cell stages, nuclei number or the segregated anaphase sister chromosomes and mitotic indexes deviated from the predicted values, and the difference increased as development advanced (Table 1). The asynchrony found at these stages by the PH3 staining was not due to irregular labeling since the PH3 patterns coincide with nuclear morphology by the SYTOX Green staining (Supporting Information Fig. 5). Half of the embryos from the same experiments were left to develop to confirm that more than 90% of the embryos developed normally up to 24 h. Therefore, we can assume that the analyzed embryos would have given rise to normal embryos if left to develop.

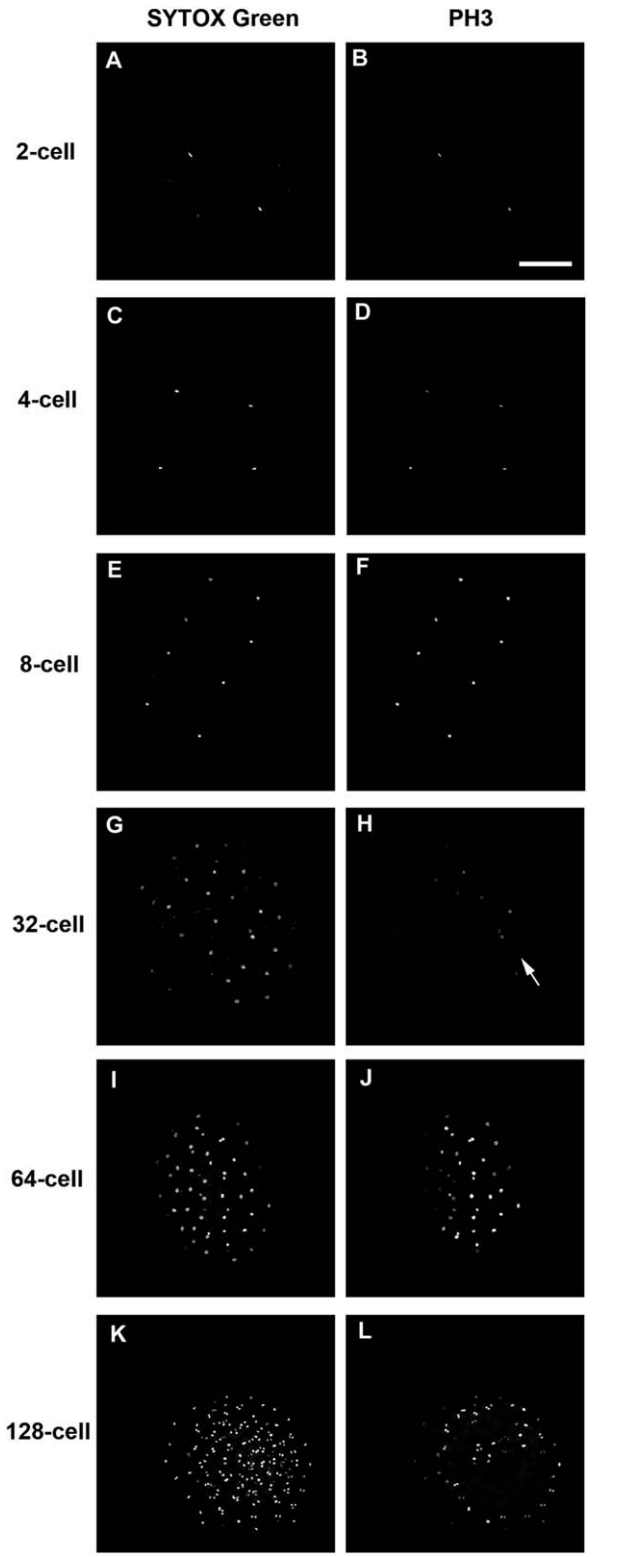


Fig. 5. Nuclei and PH3 immunofluorescence patterns during cleavage period in 2- to 128-cell stage zebrafish embryos. Animal views are shown. Small arrow indicates initiating pseudo "wave." Scale bar 200 μm in B.

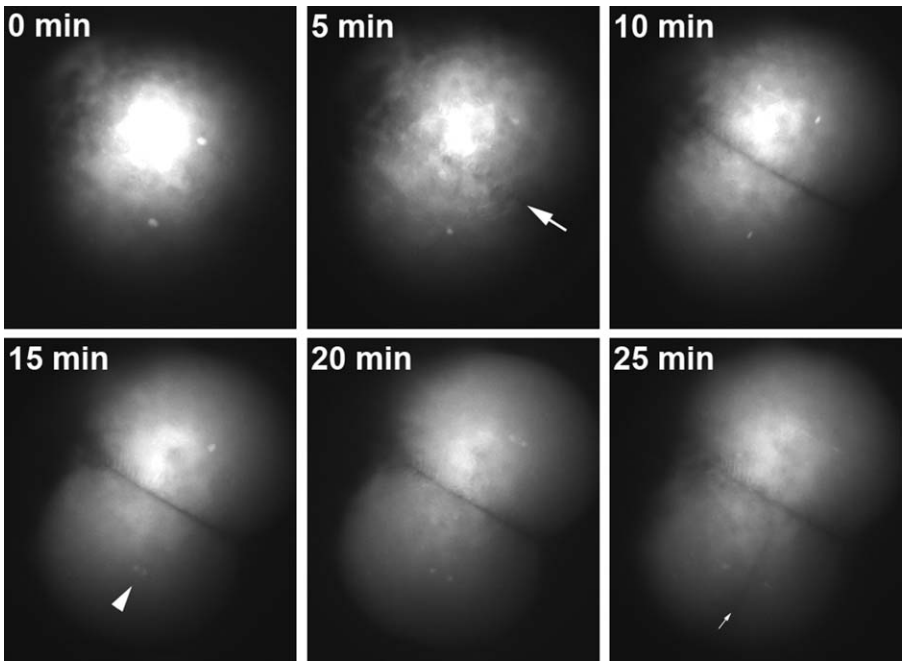


Fig. 6. Visualization of nuclei dynamics in living embryos. SYTOX Green was injected in embryos at 1 cell stage. Large arrow at 5 min indicates the first cleavage furrow. Arrowhead at 15 min indicates sister chromatids separating first in this blastomere. Small arrow at 25 min indicates cleavage furrow forming first in this blastomere.

## Cell Division Patterns at Gastrula Period

Abundant positive mitotic cells were apparent in 50%-epiboly (Fig. 1) and shield stage embryos (Fig. 8). As in the blastula embryos, we also found clusters of PH3-negative cells (asterisk in Fig. 8B).

In embryos between 80 and 90% epiboly, nuclei staining allowed us to distinguish the degree of epiboly progression of the different cell lineages. A higher density of nuclei distinctly indicated the regions in which the deep cells were located. During epiboly, these cells continue dividing; however, dorsal regions presented more abundant PH3-positive nuclei (Fig. 9A,B), possibly correlated with higher cell density. In contrast to deep cells, EVL cells stop dividing and flatten to relocate by epiboly during gastrulation (Kimmel et al., 1995). Throughout epiboly, the EVL cells and the YSL nuclei are known to advance faster than deep cells toward the vegetal pole (Solnica-Krezel, 2006); this event was confirmed by the rounded morphology and advanced position of the corresponding nuclei (Fig. 9A–F). As discussed previously, the EVL and YSL nuclei correspond to tissues of extra-embryonic destiny that enter mitotic arrest during the blastula period (Kane et al., 1992); as expected, these nuclei were PH3-negative (Fig. 9C–D).

Embryos between 90%-epiboly and bud stage distinctly presented a region with decreased cell density in the deep cell layer that expanded during epiboly (Fig. 9E, e1), corresponding to the so-called "evacuation zone" (Kimmel et al., 1995). Mitotic indexes and therefore cell proliferation in this region significantly decrease as compared to similar areas in the dorsal region (Fig. 9E and F, inserts e1,e2,f1, and f2) (Table 2).

At bud stage, deep cells are still converging dorsally, a process that is completed by somitogenesis (Fig. 2L–N). Consequently, cells that are positive for the mitosis marker appear more abundant at the dorsal side of the embryo, where somites will begin to form (Fig. 9H, arrow).

## Cell Division Patterns During Segmentation Period

Nuclei patterns in zebrafish embryos indicate that convergence to the main body is completed by the somitogenesis stages. As a consequence, the evacuation zone expands, and the embryo main body axis visibly increases in size (Fig. 10A–F). Between the 3- and 6-somite stages, cell proliferation is ubiquitous with no apparent defined patterns.

During this period, one of the most conspicuous features is tail appearance and extension (Kimmel et al., 1995). Interestingly, no apparent increase in mitotic nuclei is observed in the tail region during these stages although a general increase in PH3 positive nuclei is observed in the whole embryo possibly related to the embryo main axis extension (Figs. 9 and 10). After the 18-somite stage, tail extension is more obvious, and mitoses persist (Figs. 1 and 2). Cell proliferation remains abundant up to the 28-somite stage, when a major decrease is observed and mitoses localize more dorsally and at the very tip of the tail (Fig. 1S).

Brain rudiment sculpting occurs by the 18-somite stage, generating the regionalization of neuromeres such as the telencephalon, diencephalon, mesencephalon, and the hindbrain rhombomeres (Kimmel et al., 1995). Nuclei

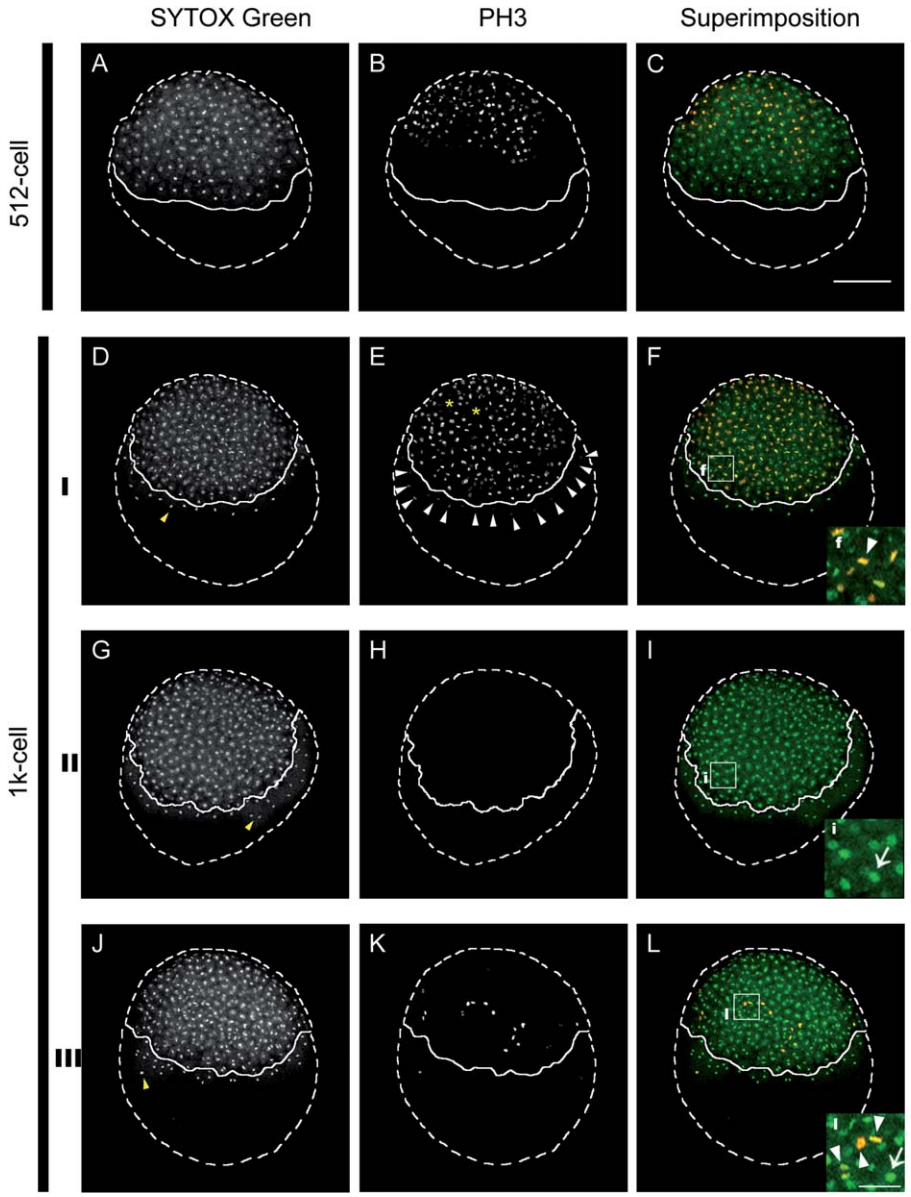


Fig. 7. Proliferation patterns in 512- (**A–C**) and 1k-cell stage zebrafish embryos (**D–L**). The punctuated line shows the contour of the embryos, and continuous lines indicate the margin between blastoderm and the yolk cell. **I:** A 1k-cell embryo showing the characteristic yolk syncytial layer (YSL) nuclei (yellow arrowhead in D), with all their nuclei positive for the PH3 marker (arrowheads in E). Asterisks in E indicate clusters of nuclei negative for the PH3 marker. Arrowhead in F insert shows a metaphase cell **II:** A 1k-cell embryo showing the blastoderm and YSL nuclei (yellow arrowhead in G) negative for the PH3 marker (H). Arrowhead in I insert shows an interphase cell. **III:** A 1k-cell embryo showing only one YSL nuclei (yellow arrowhead in J) positive for the PH3 marker (K) and scattered blastoderm cells in mitosis. Arrowhead in I insert shows an interphase cell. Arrowheads in L insert shows cell nuclei at different stages of mitosis and the arrow shows an interphase nuclei. Lateral views are shown. Nuclei are in green, PH3 marker in red. Scale bar 200 μm in C; 50 μm in L.

staining of 18-somite embryos permitted the visualization of the general structure of these brain regions, which is well-preserved (Fig. 11). In these embryos (left side view), the brain region, the eye, the otic vesicle (Figs. 11A–D), the notochord and the somites could be identified. Confocal images of the PH3 marker showed that mitoses are ubiquitous, with particular regions of decreased proliferation, particularly where the yolk cell and extension form (Figs. 11A and B, asterisk). Abundant proliferating cells were observed in the head and tail regions (Fig. 11B). Interestingly, in a dorsal view of these embryos, a two-row pattern of mitosis was evident in the neural tube along the antero–posterior axis (Fig. 11E–H).

## Cell Division Patterns After 24 h of Development

Pharyngula embryos were analyzed at approximately prim-6 (27-somite, Fig. 12) and prim 16 (28-somite, Fig. 13) stages. The nuclei pattern revealed by SYTOX Green

**TABLE 1. Nuclei number and mitotic index quantification in zebrafish embryos from 1-cell to 512-cell stage**

| Stage | Embryos analyzed[a] | Nuclei number[b] | % of embryos with expected nuclei | M.I. | % of embryos at interphase |
|---|---|---|---|---|---|
| 1-cell | 11 | 1.2 | 100 | 1 | 63.6 |
| 2-cell | 14 | 3.2 | 92.9 | 1 | 78.6 |
| 4-cell | 32 | 4.3 | 93.8 | 1 | 40.6 |
| 8-cell | 17 | 8.3 | 87.5 | 1 | 76.5 |
| 16-cell | 11 | 16.9 | 46.2 | 0.86 | 6 |
| 32-cell | 17 | 31.3 | 11.8 | 0.82 | 23.5 |
| 64-cell | 5 | 68.2 | 0 | 0.13 | 60 |
| 128-cell | 4 | 142.5 | 0 | 0.56 | 0 |
| 256-cell | 5 | 216.2 | 0 | 0.32 | 16.7 |
| 512-cell | 11 | 553.3 | 0 | 0.14 | 0 |

M.I., mitotic index.
All embryos were analyzed by confocal microscopy. What is counted as "Nuclei" actually represents nuclei or the segregated anaphase sister chromosomes counted as a group, not individually. Embryos at each stage were expected to present $2^n$ nuclei, where $n$ is the cell cycle. For example, a 4-cell embryo was expected to present 4 or 8 nuclei (see Fig. 3A and D) or groups of anaphase sister chromosomes (see Fig. 3G). However, after 2-cell stage not all embryos presented the exact number of expected nuclei. After 16-cell stage the mitotic index did not match the expected index of 1, as predicted in the classical model for embryos that present nuclei at mitosis, indicating that some nuclei were not PH3 positive.
[a]Total of embryos analyzed.
[b]Average nuclei number.

staining of prim-6 embryos revealed the general structure of the embryo in full confocal slice projections, along with more specific structures in partial confocal projections such as the eye, otic vesicle, neuromers, and somites (Fig. 12). Positive nuclei for the PH3 marker extend to the entire cephalic region as compared to 18-somite stage embryos. In a similar manner, the tail region remains, with abundant proliferating cells, with the exception of the cells covering the yolk extension, which are mostly negative (Fig. 12A,B, asterisk). Dorsal views of the neural tube of 27-somite embryos demonstrate that the two-row pattern of proliferating cells is maintained in the cells corresponding to neural tissue along the antero–posterior axis (Supporting Information Fig. 6), as previously observed in 18-somite embryos (Fig. 12E,F, inserts g and h).

Nuclei staining of 28-somite embryos demonstrated the advance in general embryo morphology sculpting, particularly in organs such as the eye, otic vesicle, and brain (Fig. 13A–D). Cell proliferation is abundantly distributed in the whole embryo, with some interesting specific patterns. For example, the midbrain shows abundant mitotic nuclei in the ventral region as compared to the dorsal side. The cerebellum shows abundant mitotic nuclei in the most posterior region as compared to the anterior portion. The tail shows abundant proliferating cells, with a marked difference in the tail region posterior to the yolk extension, where mitoses are concentrated in the dorsal side and less abundant in the ventral fin. Interestingly, the cloaca anlagen shows distinctive mitotic nuclei as compared to the surrounding tissues (Fig. 13A and B, arrow). Mitotic nuclei were observed in tail myotomes (Fig. 13E and F, arrowheads) in both lateral and coronal slices of full confocal projections. In general, mitotic nuclei are present in the mesodermal tissue, with the exception of the notochord and the yolk extension (Fig. 13e and f).

## DISCUSSION

The present work describes the patterns and dynamics of mitosis during the first day of zebrafish development. The dynamics of cell divisions and the cell cycle have been presented previously (Kane et al., 1992; Kane and Kimmel, 1993; Kimmel et al., 1995; Olivier et al., 2010). However, our study is the first to analyze the immunolocalization patterns of a mitosis marker in zebrafish embryos. This simple but powerful approach revealed novel patterns of cell proliferation that occur in normal developing embryos and are different from those predicted by the current models of early development. In the following sections, we discuss the most notable findings and present possible explanations for the differences identified.

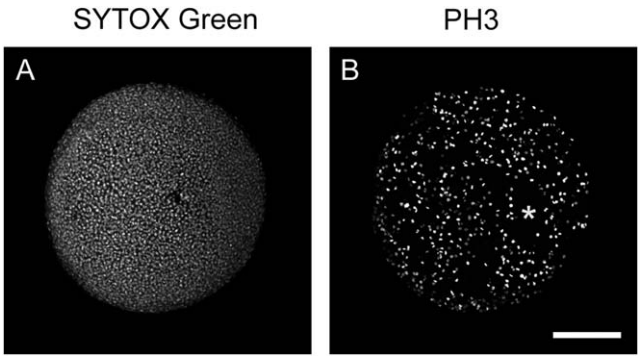


Fig. 8. Proliferation patterns in shield stage embryos. Animal pole views are shown in all images. (**A** and **B**) maximal intensity projection of a complete *z*-series image set of a shield stage embryo. Asterisks indicate blastoderm regions where nuclei are negative for the PH3 marker. 200 μm scale bar.

### Mitosis Synchronization is Lost Before the Midblastula Transition in Zebrafish

In many animals, after fertilization, the zygote is divided by rapid cleavages, generating numerous blastomeres. Classical studies in zebrafish have indicated that cleavages during the first 10 cell cycles occur in a highly stereotyped and synchronous fashion until embryos

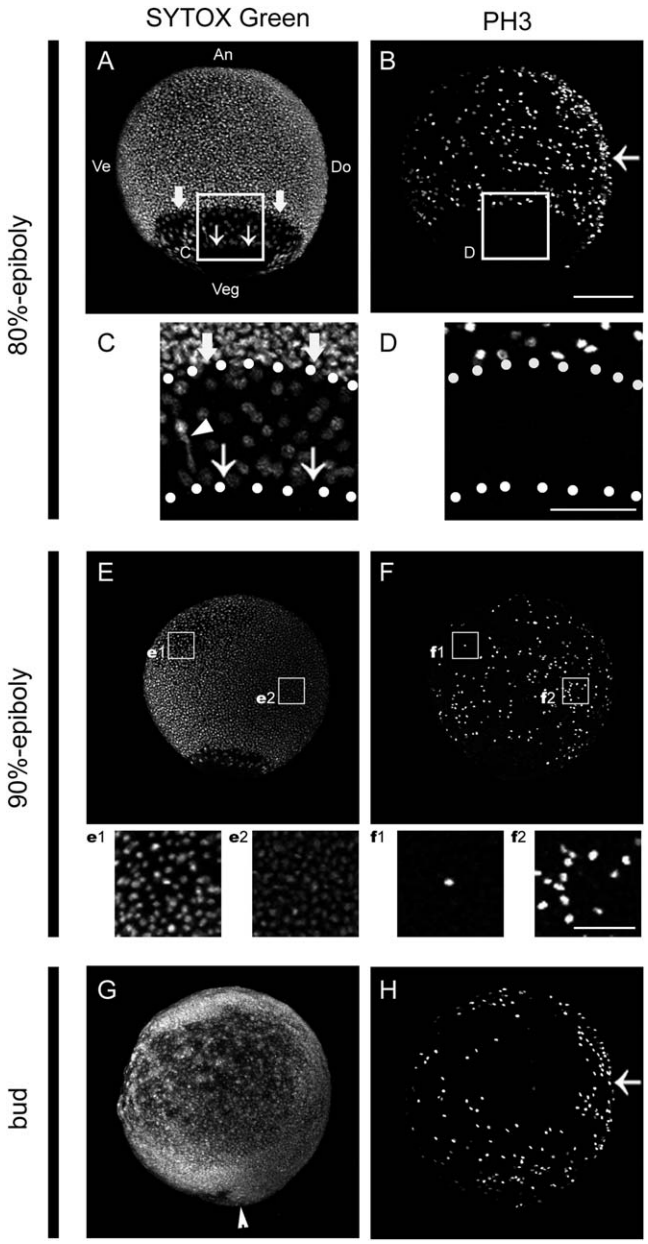


Fig. 9. Proliferation patterns of zebrafish embryos from 80%-epiboly to bud stage. (**A–D**) 80%-epiboly embryo. White thick arrows in A and C indicate the migration front of deep cells, and white thin arrows indicate the migration front of enveloping layer cells. White arrow in (B) indicates the dorsal side with abundant PH3 positive nuclei as compared to the ventral side. (**C**, **D**) Amplification of inserts indicated in A and B highlighting the migration front difference between blastoderm lineages. In C white arrowhead indicates an extended nuclei. (**E**, **F**) 90%-epiboly embryo. (**e1-f2**) Amplification of inserts indicated in E and F. These images highlight the differences in nuclei and mitotic densities in two different embryo regions (ventral and dorsal) at 90%-epiboly. Notice that inserts e1 and f1 correspond to the evacuation zone region. (**G**, **H**) Bud stage embryo. In (G) white arrowhead indicates the region where the tail bud will form and white arrow in (H) indicates the embryo dorsal side with abundant PH3 positive nuclei. An, animal pole; Veg, vegetal pole; D, dorsal side; V, ventral side. 200 μm scale bar in B, for A, E, F, G and H. 100 μm scale bar in D. 50 μm scale bar in f2 for e1, e2, and f1.

**TABLE 2. Nuclei count and mitotic indexes in ventral evacuation zone and dorsal region of 70–90% epiboly embryos**

| | Embryos analyzed[a] | Nuclei | | Mitotic index | |
|---|---|---|---|---|---|
| | | Number[b] | SD | M.I. | SD |
| Evacuation zone | 5 | 103 | 10.3 | 0.02 | 0.02 |
| Dorsal region | 5 | 150.2 | 9 | 0.12 | 0.04 |

M.I., average mitotic index; SD, standard deviation.
Regions of interest are equivalent to e1, e2, f1, and f2 shown in Fig. 9, were used for quantification.
[a]Total of embryos analyzed.
[b]Average nuclei number.

enter the MBT (Kane and Kimmel, 1993). Recent studies reported that the cell cycle and cleavage begin to drift out of synchrony in the transition of the 4- to 8-cell stage (Olivier et al., 2010). Surprisingly, none of these studies have employed molecular markers to confirm the degree of cell synchrony during entry into mitosis. In the early studies, DNA staining with Hoechst, which was used to characterize mitotic cycles on whole mounts in *Drosophila* during the 1980s (Foe and Alberts, 1983), could have been used, while more recent studies could have taken advantage of the well-established phosphorylation of histone H3 originally described in the 1990s (Hendzel et al., 1997). Our results from the immunolocalization and visualization by confocal microscopy and immunohistochemistry suggested that metasychrony begins in some embryos at the two-cell stage, although the two methods presented some discrepancies. While immunohistochemistry indicated that PH3 is asymmetric in ~10% of the two-cell stage embryos in mitosis (Fig. 4), the confocal images did not reveal this sharp distinction among blastomeres (Fig. 5), although slight differences in the intensities of the signal were evident in some cases. The dissimilarity could be due in part to the differences in the processing and visualization of the tissues, which may have yielded differences in sensitivity. For this reason, we performed *in vivo* tracking of nuclei dynamics by staining DNA with SYTOX Green. The tracking experiments yielded additional evidence that blastomere mitotic metasynchrony begins at the two-cell stage (Fig. 6), earlier than recently reported by Olivier et al. Our results confirm that metasynchronous two-cell stage embryos are capable to develop at least up to 30% epiboly; however, the early exposure to fluorescence or intense laser illumination required either for confocal or multi photon microscopy negatively affect development. Further experiments are required to confirm that asynchrony occurs in unmanipulated embryos and to precisely determine their frequency and impact on development. For this purpose a transgenic line expressing an enhanced version of GFP fused to the histone H2B would be appropriate. Between the 1- and 8-cell stages, the majority of the embryos exhibited a nuclei number and mitotic index that were in agreement with those expected for a period of synchronous cell division. By contrast, after the 16-cell stage, the projected $2^n$ nuclei number and 1 or 0 mitotic indexes substantially diverged from the predicted values. Interestingly, the percentage of embryos with the predicted nuclei

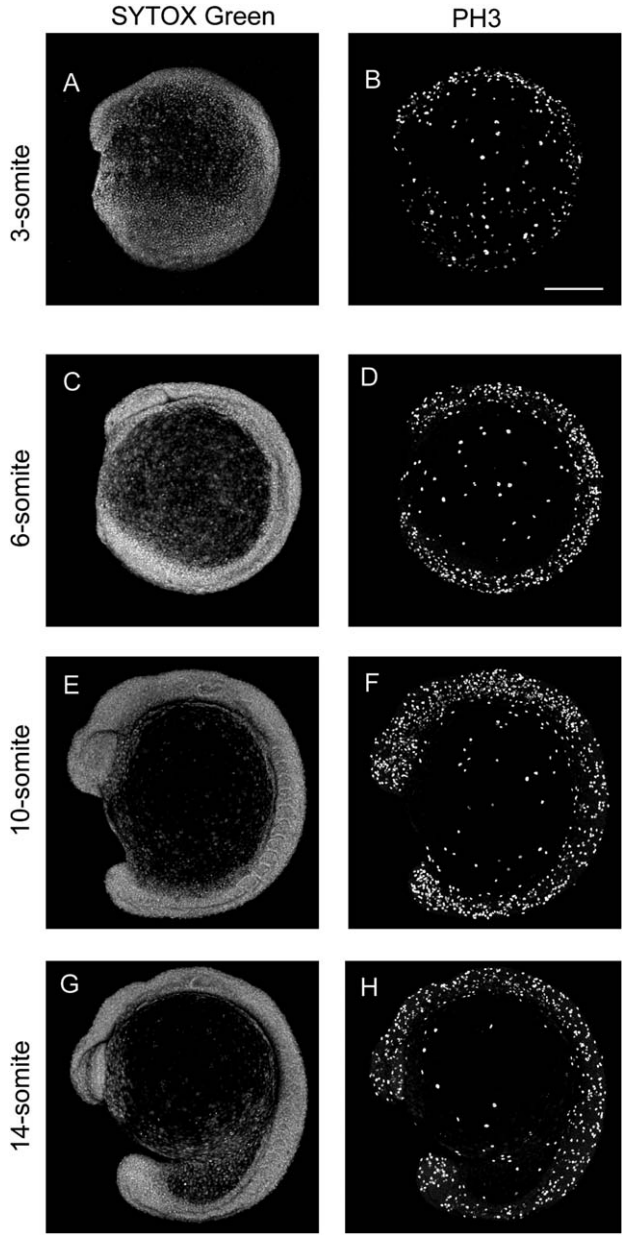


Fig. 10. Proliferation patterns from 3- to 14-somite stage embryos. (**A**, **B**) 3-somite stage embryo. (**C**, **D**) 6-somite stage embryo. (**E**, **F**) 10-somite stage embryo. (**G**, **H**) 14-somite stage embryo. Lateral views. 200 μm scale bar in B.

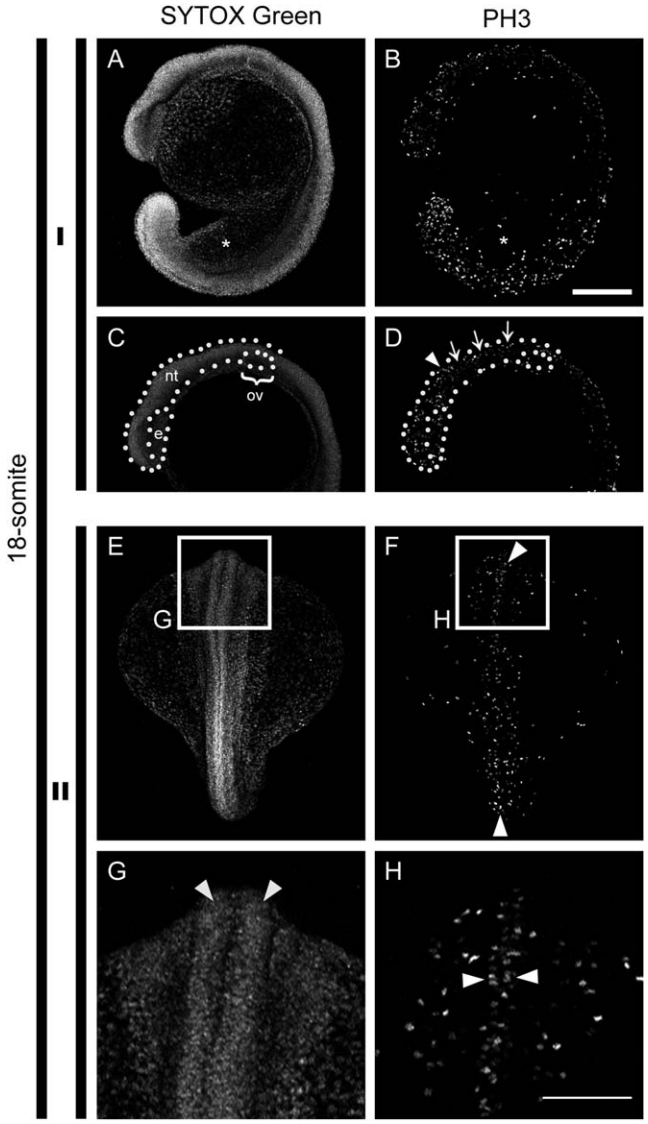


Fig. 11. Proliferation patterns in 18-somite stage embryos. **I:** Left side views of 18-somite embryos. **II:** Dorsal views of 18-somite embryos. (**A**, **B**) Full confocal slice projections. Asterisk indicates the yolk extension. (**C**, **D**) Partial confocal slice projections where most superficial slices were omitted to highlight internal patterns. White doted lines highlight different structures like the eye (e), neural tube (nt), and otic vesicle (ov). In D, the arrowhead indicates the border between mesencephalon and rhombencephalon and the arrows mark rhombomeres limits. (**E**, **H**) Dorsal view of 18-somite stage embryo. The embryo shows abundant PH3 positive nuclei in the main axis as compared to the yolk cell (H). (**G**, **H**) Amplification of corresponding inserts shown in E and F to highlight the dorsal region of the neural tube (white arrowheads), that shows mitotic nuclei arranged in two rows along the antero–posterior length of the embryo. 200 μm scale bar in B. 100 μm scale bar in H.

numbers declined as development advanced. Beginning with the 64-cell stage, we did not find any embryo that matched the predicted number. Most previous reports have averaged the results from the embryos analyzed and presented prototypes of development. In the present study, if we take into account only the average number of nuclei at each stage and compare it with the theoretical number, the correlation coefficient is high (0.99), behaving as expected. However, when the embryos are considered individually, the variability in early development becomes evident and is not represented by the reported prototypes. In addition, we found that the mitotic index steadily declined after the 8-cell stage. Taken together, our findings indicate that early development is less synchronous than anticipated and that synchrony is not a requirement for proper development in zebrafish.

The higher level of synchronization observed before the 8-cell stage can be explained in part because early

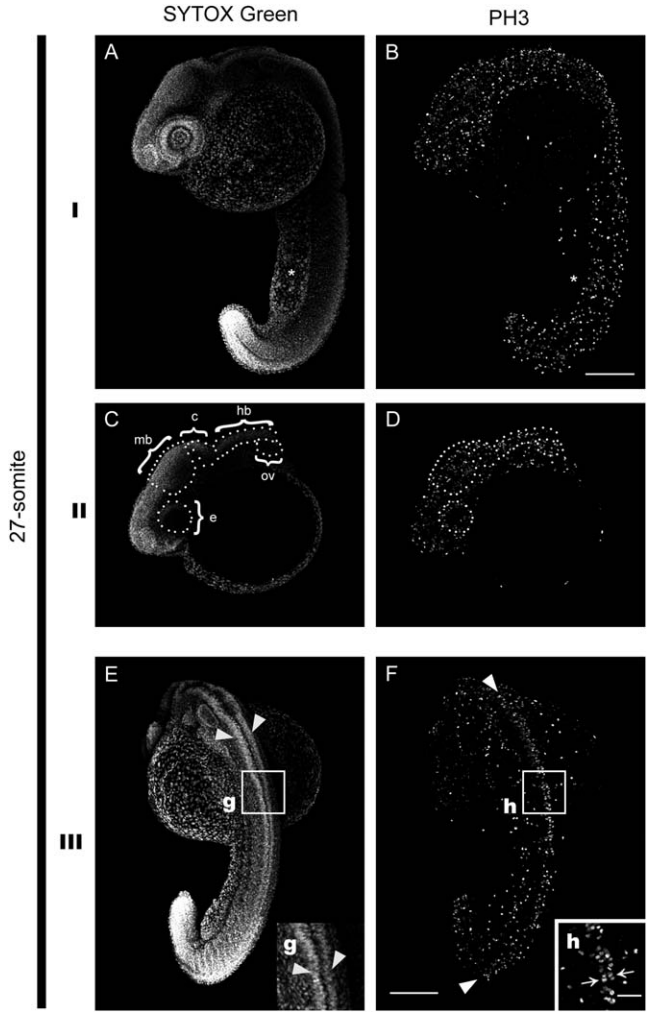


Fig. 12. Proliferation patterns in 27-somite stage embryos. **I:** Left-side views. **II:** Partial projections were most superficial slices were omitted to highlight internal patterns. **III:** Dorsal views. The embryo shows abundant PH3 positive nuclei in the main axis as compared to the yolk cell. The dorsal region of the neural tube (white arrowheads) shows mitotic nuclei arranged in two rows along antero–posterior length of the embryo as in the previous stage analyzed. (**g, h** inserts)**:** show an amplification to highlight the structure and proliferation patterns in the neural tube. e, eye; mb, midbrain; c, cerebellum; hb, hindbrain; ov, otic vesicle. 200 μm scale bar in B. 50 μm scale bar in h insert.

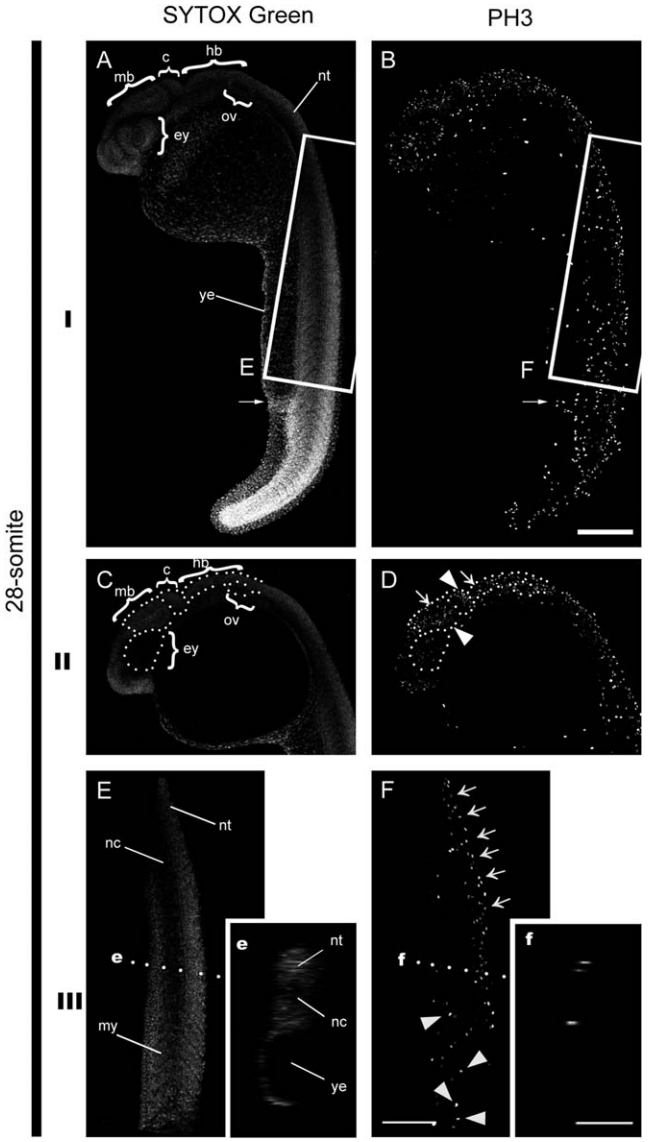


Fig. 13. Proliferation patterns in 28-somite stage embryos. **I:** Full confocal slice projections of an entire embryo. **II:** Partial confocal slice projections of the brain region. White doted lines highlight structure like the eye (ey), midbrain (mb), cerebellum (c), hindbrain (hb), and otic vesicle (ov). White arrowheads in D indicate mitotic nuclei in midbrain and hindbrain. White arrows indicate regions with less abundant mitotic nuclei in brain regions. **III:** Partial projections of the tail region show structures corresponding to the notochord (nc) and myotomes (my). (**e** and **f**) Inserts show sagital sections of images indicated in images E, F by the white dotted lines. Notice the positive nuclei for PH3, except in the corresponding notochord and yolk extension. ey, eye; mb, midbrain; hb, hindbrain; c, cerebellum; nt, neural tube; ye, yolk extension. 200 μm scale bar in B. 100 μm scale bar in f insert.

cleavages are meroblastic in zebrafish, and thus, the blastodisc is only partially divided; blastomeres remain bridged among them and the underlying yolk. Blastomere bridging in early zebrafish embryos is known to permit the passage of small molecules, which are more commonly observed among lineage-related blastomeres (Kimmel and Law, 1985). Indeed, cell–cell communication by passage of low molecular weight molecules and second messengers through intercellular bridges and gap junctions has long been known to participate in cell cycle synchronization in different cell types (Schultz, 1985; Guthrie and Gilula, 1989; Levin, 2007), a mechanism that may be responsible for the higher coordination in cleavage and mitosis during the first three cell cycles. At later stages, in particular at the 16-cell stage, cleavage is completed, and the four most central blastomeres are individualized, leaving the remaining 12 marginal blastomeres connected to the yolk (Kimmel et al., 1995). The difference in connectivity among blastomeres may explain why from this stage both the nuclei number and mitotic index drift notably as compared to previous stages (Table 1), but the precise mechanism remains to be determined. Alternatively, other mechanisms may

account for this asynchrony, like an intrinsic cell cycle temporal variability or an interphase versus mitosis length differences among blastomeres. By the 64-cell stage, cleavage planes are more irregular, complicating cell quantification by light microscopy (Kimmel and Law, 1985). Variability in development among embryos has long been known to occur normally even when the embryos are obtained from a single clutch, fertilized simultaneously *in vitro* or taken from clonal strains with more genetic uniformity (Streisinger et al., 1981; Kimmel et al., 1995).

We found embryos from the 1- to 1k-cell stage that were synchronized at interphase. Nonetheless, after the 128-cell stage, these embryos were observed less frequently, perhaps because interphase also eventually became asynchronous. However, interphase molecular markers should be tested to determine the degree of asymmetry and synchronization before the MBT.

## Mitotic Clusters Before the Midblastula Transition

Another important observation is the presence of mitotic clusters or domains with apparent clonal coordination at interphase in 512- and 1k-cell stage (Fig. 7B,E,K) and shield-stage embryos (Fig. 8), in agreement with the recent report by Olivier et al. (2010) that clones originated by the first eight blastomeres remain clustered up to the 512-cell stage. These patterns of proliferation occurred simultaneously with the mitotic pseudo "waves." The evidence of these domains could indicate that mitosis synchronization or metasynchronization is occurring at two levels: at the level of the whole blastoderm with a pattern of propagation from the animal to vegetal pole as well as a more local synchronization among neighbor blastomeres related by lineage. The mechanisms responsible for the coordination of both levels of mitotic coordination remain to be identified; however, this coordination is likely regulated by signaling mechanisms that are propagated among cells.

## Cell Proliferation Versus Migration in Early Development

In zebrafish, during the cleavage period, the blastomeres divide extremely fast at 15- to 19-min intervals (Kane and Kimmel, 1993; Olivier et al., 2010). This rapid cell division lacks G1 and G2 phases and is composed exclusively of S and M phases (Budirahardja and Gonczy, 2009). After the MBT, the G1 and G2 phases are acquired (Zamir et al., 1997; Dalle Nogare et al., 2009). Simultaneously, cells begin to show signs of motility by extending pseudopods during interphase, in contrast to cells undergoing mitosis, which take spherical shapes and do not present signs of pseudopod formation (Kane and Kimmel, 1993). Rapid cleavages, which are characteristic of early development in various animal species, may be required to reach the critical cell numbers needed for proper embryogenesis; cell migration initiates only after such numbers are reached. In *Xenopus* embryos, the MBT also marks the onset of embryonic transcription and cell motility; however, if explants of these embryos are treated with cell cycle inhibitors, transcription is activated before the MBT, and cells become migratory (Kimelman et al., 1987). In addition, inhibition of cell proliferation before the onset of gastrulation in *Xenopus* causes severe developmental defects, whereas inhibition after the beginning of gastrulation produces mild morphological alterations (Cooke, 1973a,b). Our results demonstrate that abundant proliferation occurs in embryos during early development (Figs. 1–8); then, after the shield-stage, we found embryos in which cell proliferation appeared to decrease in tissues with considerable cell migration, such as the involuting cells at the shield. Therefore, although we did not address this point directly, some of the patterns we found are consistent with evidence suggesting that cells undergoing active migration decrease their proliferation rate considerably. Such patterns include the EVL cells at 80%-epiboly (Fig. 9A–F) or the deep cells of the ventral blastoderm, which compared to the dorsal cells in embryos at 90%-epiboly (Fig. 9E and F and inserts e1 to f2), present decreased PH3 staining.

This phenomenon has been reported to occur in different developing tissues. For example, in *Xenopus*, the paraxial mesodermal cells transiently stop dividing, and this cessation is required for the proper positioning of the paraxial mesoderm by convergence and extension (Leise and Mueller, 2004). Similarly, in zebrafish, we show evidence for a mitotic decrease in the EVL and the YSL in embryos between 80 and 90%-epiboly. The faster epiboly in these lineages compared to deep cells could be attributable to the mitotic arrest.

## Cell Proliferation in Different Embryonic Organs and in the Tail

In the present study, we found that cell proliferation accompanies the appearance of different organ anlages such as the eye, the otic vesicle, the tail (Figs. 10 and 11) and the neuromeres during the sculpting of the brain (Figs. 11 and 12). In the brain, proliferation is abundant and ubiquitous up to the 18-somite stage. Thereafter, interesting patterns arise, for instance, the parallel rows that line up the most axial regions of the neural tube along the antero–posterior axis (Figs. 11, 12, and Supporting Information Fig. 6) or the dorso–ventral and antero–posterior differences that were, respectively detected in the midbrain and cerebellum at the prim-16 stage. However, the significance of these patterns needs to be explored, given that in other vertebrates, such as *Xenopus*, experimental inhibition of proliferation at the beginning of gastrulation does not interfere significantly with the development of homologous embryonic structures, demonstrating that morphogenesis can occur even in the absence of proliferation (Harris and Hartenstein, 1991). It has been proposed that proliferation in these regions participates mainly in the achievement of the proper size rather than in morphogenesis (Saka and Smith, 2001). This proposal remains to be proven experimentally in zebrafish.

We have also found that, during initial tail formation and during the physical separation of the tail from the yolk cell, cell proliferation is abundant with no major changes (Figs. 1 and 10–13). The caudal cell movement of dorso-medial region cells of the tailbud has also been implicated as one of the main driving forces for tail elongation in zebrafish (Kanki and Ho, 1997). However, how these events (cell proliferation and migration) and yolk morphogenesis contribute to tail individualization and

projection should be analyzed in greater detail by *in vivo* cell tracking and advanced microscopy techniques.

## CONCLUDING REMARKS

In summary, we made several findings in the present study. We obtained evidence for an initial blastomere mitotic drift at the two-cell stage that increases in subsequent cell divisions. We also found evidence that mitotic synchrony is lost at the molecular level, well before the MBT. We described the occurrence of simultaneous patterns of proliferation, clusters, and pseudo "waves," which appear to be coordinated in early development. The degree of complementarity between different cell behaviors remains to be described and analyzed in detail in zebrafish to gain a more global view of their contribution to normal development, a task that is in progress in our group. Finally, we presented a series of the normal patterns of mitosis during the first day of zebrafish embryo development that we believe will serve as a development table reference for comparative analysis. In fact, we are currently building a database for the patterns of occurrence of different cell behaviors in early zebrafish development in which average or representative images are presented as well as the variability that normally occurs during development.

## ACKNOWLEDGEMENTS

The authors thank Dulce I. Pacheco-Benítez and Laura S. Ramirez-Angeles for technical support with the animal care and Andres Saralegui for support with the confocal microscope.

## LITERATURE CITED

Abramoff MD, Magelhaes PJ, Ram SJ. 2004. Image Processing with ImageJ. Biophotonics Int 11:36–42.

Budirahardja Y, Gonczy P. 2009. Coupling the cell cycle to development. Development (Cambridge, England) 136:2861–2872.

Cooke J. 1973a. Morphogenesis and regulation in spite of continued mitotic inhibition in Xenopus embryos. Nature 242:55–57.

Cooke J. 1973b. Properties of the primary organization field in the embryo of Xenopus laevis. IV. Pattern formation and regulation following early inhibition of mitosis. J Embryol Exp Morphol 30:49–62.

D'Amico LA, Cooper MS. 2001. Morphogenetic domains in the yolk syncytial layer of axiating zebrafish embryos. Dev Dyn 222: 611–624.

Dalle Nogare DE, Pauerstein PT, Lane ME. 2009. G2 acquisition by transcription-independent mechanism at the zebrafish midblastula transition. Dev Biol 326:131–142.

Edgar BA, O'Farrell PH. 1989. Genetic control of cell division patterns in the Drosophila embryo. Cell 57:177–187.

Foe VE. 1989. Mitotic domains reveal early commitment of cells in Drosophila embryos. Development (Cambridge, England) 107:1–22.

Foe VE, Alberts BM. 1983. Studies of nuclear and cytoplasmic behaviour during the five mitotic cycles that precede gastrulation in Drosophila embryogenesis. J Cell Sci 61:31–70.

Guthrie SC, Gilula NB. 1989. Gap junctional communication and development. Trends Neurosci 12:12–16.

Harris WA, Hartenstein V. 1991. Neuronal determination without cell division in Xenopus embryos. Neuron 6:499–515.

Hendzel MJ, Wei Y, Mancini MA, Van Hooser A, Ranalli T, Brinkley BR, Bazett-Jones DP, Allis CD. 1997. Mitosis-specific phosphorylation of histone H3 initiates primarily within pericentromeric heterochromatin during G2 and spreads in an ordered fashion coincident with mitotic chromosome condensation. Chromosoma 106:348–360.

Ikegami R, Zhang J, Rivera-Bennetts AK, Yager TD. 1997. Activation of the metaphase checkpoint and an apoptosis programme in the early zebrafish embryo, by treatment with the spindle-destabilising agent nocodazole. Zygote (Cambridge, England) 5: 329–350.

Kane DA, Kimmel CB. 1993. The zebrafish midblastula transition. Development (Cambridge, England) 119:447–456.

Kane DA, Warga RM, Kimmel CB. 1992. Mitotic domains in the early embryo of the zebrafish. Nature 360:735–737.

Kanki JP, Ho RK. 1997. The development of the posterior body in zebrafish. Development (Cambridge, England) 124:881–893.

Keller PJ, Schmidt AD, Wittbrodt J, Stelzer EH. 2008. Reconstruction of zebrafish early embryonic development by scanned light sheet microscopy. Science 322:1065–1069.

Kimelman D, Kirschner M, Scherson T. 1987. The events of the midblastula transition in Xenopus are regulated by changes in the cell cycle. Cell 48:399–407.

Kimmel CB, Ballard WW, Kimmel SR, Ullmann B, Schilling TF. 1995. Stages of embryonic development of the zebrafish. Dev Dyn 203:253–310.

Kimmel CB, Law RD. 1985. Cell lineage of zebrafish blastomeres. I. Cleavage pattern and cytoplasmic bridges between cells. Dev Biol 108:78–85.

Leise WF, III, Mueller PR. 2004. Inhibition of the cell cycle is required for convergent extension of the paraxial mesoderm during Xenopus neurulation. Development (Cambridge, England) 131:1703–1715.

Levin M. 2007. Gap junctional communication in morphogenesis. Prog Biophys Mol Biol 94:186–206.

Murphey RD, Stern HM, Straub CT, Zon LI. 2006. A chemical genetic screen for cell cycle inhibitors in zebrafish embryos. Chem Biol Drug Des 68:213–219.

Olivier N, Luengo-Oroz MA, Duloquin L, Faure E, Savy T, Veilleux I, Solinas X, Debarre D, Bourgine P, Santos A, Peyrieras N, Beaurepaire E. 2010. Cell lineage reconstruction of early zebrafish embryos using label-free nonlinear microscopy. Science 329: 967–971.

Saka Y, Smith JC. 2001. Spatial and temporal patterns of cell division during early Xenopus embryogenesis. Dev Biol 229:307–318.

Salas-Vidal E, Lomeli H. 2004. Imaging filopodia dynamics in the mouse blastocyst. Dev Biol 265:75–89.

Schultz RM. 1985. Roles of cell-to-cell communication in development. Biol Reprod 32:27–42.

Solnica-Krezel L. 2006. Gastrulation in zebrafish—all just about adhesion? Curr Opin Genet Dev 16:433–441.

Streisinger G, Walker C, Dower N, Knauber D, Singer F. 1981. Production of clones of homozygous diploid zebra fish (Brachydanio rerio). Nature 291:293–296.

Sulston JE, Schierenberg E, White JG, Thomson JN. 1983. The embryonic cell lineage of the nematode Caenorhabditis elegans. Dev Biol 100:64–119.

Urbani L, Sherwood SW, Schimke RT. 1995. Dissociation of nuclear and cytoplasmic cell cycle progression by drugs employed in cell synchronization. Exp Cell Res 219:159–168.

Zamir E, Kam Z, Yarden A. 1997. Transcription-dependent induction of G1 phase during the zebra fish midblastula transition. Mol Cell Biol 17:529–536.

Zhang L, Kendrick C, Julich D, Holley SA. 2008. Cell cycle progression is required for zebrafish somite morphogenesis but not segmentation clock function. Development (Cambridge, England) 135:2065–2070.